

Direct-focusing surface-emitting laser: supplement

KAZUYOSHI HIROSE,* HIROKI KAMEI, AND TAKAHIRO SUGIYAMA

Central Research Laboratory, Hamamatsu Photonics K. K., 5000 Hirakuchi, Hamakita-ward, Hamamatsu, Shizuoka, Japan

**hirose-ka@crl.hpk.co.jp*

This supplement published with Optica Publishing Group on 14 January 2022 by The Authors under the terms of the [Creative Commons Attribution 4.0 License](https://creativecommons.org/licenses/by/4.0/) in the format provided by the authors and unedited. Further distribution of this work must maintain attribution to the author(s) and the published article's title, journal citation, and DOI.

Supplement DOI: <https://doi.org/10.6084/m9.figshare.18095882>

Parent Article DOI: <https://doi.org/10.1364/OE.447537>

Direct-focusing surface-emitting laser: supplemental document

KAZUYOSHI HIROSE,* HIROKI KAMEI, AND TAKAHIRO SUGIYAMA

Central Research Laboratory, Hamamatsu Photonics K. K., 5000 Hirakuchi, Hamakita-ward,
Hamamatsu, Shizuoka, Japan

*hirose-ka@crl.hpk.co.jp

S1 2D & 3D beam patterns

According to the theory of diffraction, 2D and 3D beam patterns can be considered as cases of Fraunhofer diffraction (2D) and Fresnel diffraction (3D), respectively [1,2]. These phenomena are formulated as follows:

$$2D: \quad U_o(x, y) = \frac{e^{j\frac{2\pi}{\lambda}z} e^{j\frac{\pi}{\lambda z}(x^2+y^2)}}{j\lambda z} \iint U_i(\xi, \eta) \cdot e^{-j\frac{2\pi}{\lambda z}(\xi x + \eta y)} d\xi d\eta, \quad (S1)$$

$$3D: \quad U_o(x, y) = \frac{e^{j\frac{2\pi}{\lambda}z} e^{j\frac{\pi}{\lambda z}(x^2+y^2)}}{j\lambda z} \iint \left\{ U_i(\xi, \eta) \cdot e^{j\frac{\pi}{\lambda z}(\xi^2 + \eta^2)} \right\} \cdot e^{-j\frac{2\pi}{\lambda z}(\xi x + \eta y)} d\xi d\eta, \quad (S2)$$

where $U_o(x, y)$ is the complex EM field in the output plane, $U_i(\xi, \eta)$ is the complex EM field in the input plane, λ is the wavelength, z is the propagation distance, (x, y) denotes the orthogonal coordinate system in the output plane, and (ξ, η) denotes the orthogonal coordinate system in the input plane [1]. Regarding the integral terms, the one in Eq. S1 is a Fourier transform consisting of a linear combination of plane waves with wavevector $k = (2\pi/\lambda)(\xi, \eta)$. In contrast, the integral term in Eq. S2 is a linear combination of parabolically distorted plane waves with the same wavevector k .

S2 Fabrication process

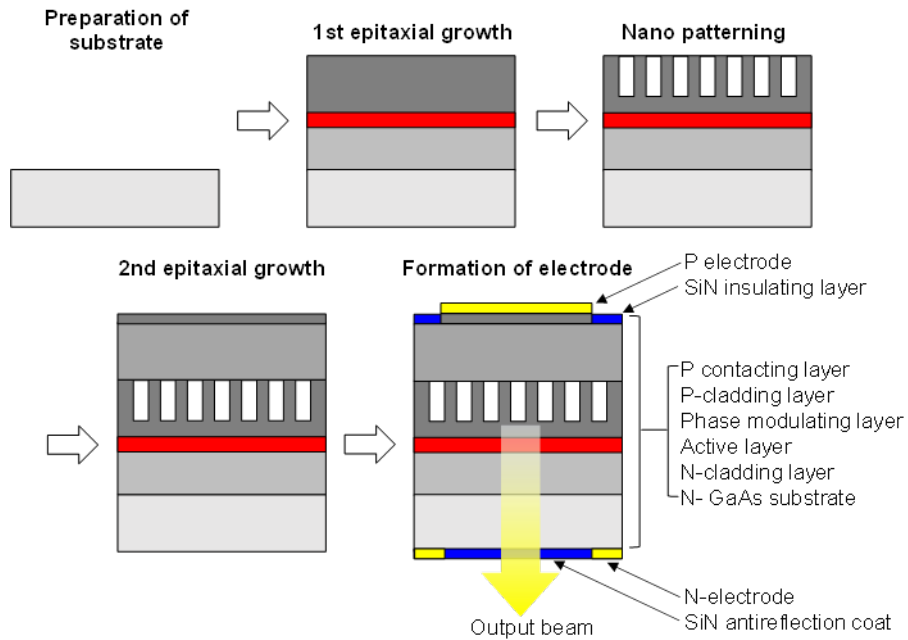


Fig. S1 Fabrication process of the iPMSEL.

S3 Hole-shifting method in regime of detour phase method

As discussed in section 2.1, the hole-shifting method illustrated in Fig. 3(a) is derived from the detour phase method, proposed in 1966. The fundamental idea of this method is to modulate the complex EM field with a spatial filter placed at the Fourier plane in order to form a 2D beam projection. The modulations of the phase and the amplitude terms are achieved by shifting the position and size of a locally open aperture in the filter [3]. Because the EM field in the near-field plane is connected to the far-field plane by Fraunhofer diffraction, which is mathematically a Fourier transform, the positional shift of the holes can be treated as the phase shift in the detour phase method. Moreover, the manner of phase modulation clearly depends on the actual positional shift of the holes. The detailed phase distribution of the in-plane light wave was discussed in a previous work [4]. The phase modulation of the output beam can be formulated as a series expansion of a light wave with an ideal phase distribution $\exp\{i\phi(x,y)\}$, as follows:

$$\Delta\phi(x,y) = \sum_{m=-\infty}^{\infty} C_m \cdot \exp\{im\phi(x,y)\}, \quad (\text{S3})$$

where $\Delta\phi(x,y)$ is the phase modulation of the diffracted in-plane light waves in the surface-normal direction due to the in-plane positionally shifted holes, m ($m = 0, \pm 1, \pm 2, \dots$) is the order of the diffraction, and C_m is the coefficient of the m th-order diffraction. The coefficient C_m depends on the manner of the positional shift, or the shape of the holes, and so on; however, the output beam, which is based on the ± 1 st-order diffraction, is considered to have an ideal phase distribution ranging from 0 to 2π even if the positional shift of the holes is not large. This is a distinctive feature of phase modulation in the in-plane lasing cavity. Moreover, the strong 0th-order out-of-plane diffraction is prevented at the M-point band edge, which is the nature of the diffraction in M-point band edge [5].

S4 Phase distribution for focusing beam

For focusing, we simply control the phase distribution conditions at the phase-modulating layer so that surface-normal incident light waves in that layer have the same optical length at the focus, which is the ordinary condition of a flat lens. This is achieved by replacing the conventional phase term ϕ_p for a 2D beam pattern with the phase term ϕ_f for focusing, which is formulated as follows:

$$\phi_f(x,y) = \pm \frac{2\pi}{\lambda} \left(\frac{a}{r} \right) \left(\sqrt{x^2 + y^2 + f^2} - f \right), \quad (\text{S4})$$

where λ is the wavelength, a is the lattice constant, r is the distance between the hole center and the lattice point, (x,y) denotes the orthogonal coordinates in the input plane, and f is the focal length. Note that the positive and negative forms of the equation correspond to concave and convex lenses, respectively. For this work, the parameters were set as $\lambda = 940$ nm, $a = 202$ nm, $r = 0.08a$, and $f = 4$ mm. The correction term $(a/r) = 12.5$ was included to correct the difference between the detour phase based on the actual positional shift (see Fig. 2(b)) and an ideal one; however, the correction term later proved unnecessary because the measured focal length was around $310 \mu\text{m}$, which was much smaller than 4 mm.

Next, we explain the deviation of the focal length. Because (x,y) coordinates in the $200 \mu\text{m} \times 200 \mu\text{m}$ emission area are sufficiently smaller than the focal length f , Eq. S3 can simply be approximated as

$$\phi_f(x,y) \approx \pm \frac{2\pi}{\lambda} \left(\frac{a}{r} \right) \frac{x^2 + y^2}{2f} = \pm \frac{2\pi}{\lambda} \frac{x^2 + y^2}{2f'}, \quad (\text{S5})$$

$$f' = f / (a/r). \quad (\text{S6})$$

The quadratic phase term in Eq. S5 has the same form as the phase term for the basic component of light waves in Fresnel diffraction (see Eq. S2), provided that the phase distribution can also be considered as the simplest form of Fresnel diffraction. Accordingly, the equivalent focal length f' was obtained as 320 μm , which agreed well with the measured focal length. Therefore, the correct formulation of the phase distribution for focusing was obtained as

$$\phi_f(x, y) = \pm \frac{2\pi}{\lambda} \left(\sqrt{x^2 + y^2 + f^2} - f \right). \quad (\text{S7})$$

It is important to note that 2π modulation is achieved when the actual positional shift of the holes, r , ranges from $-0.08a$ to $0.08a$, which seems to correspond to the phase shift ranging from -0.23π to 0.23π . This should be considered as a series expansion of the ideal phase function even for a 3D beam pattern, as with a 2D beam pattern [4].

S5 Focal spot size of diffraction limit

A projection pattern at the focal plane of an ideal lens is considered as Fraunhofer diffraction of the incident pattern at the lens' entrance aperture, because the quadratic phase term for Fresnel diffraction (Eq. S2) cancels out the phase of the lens (Eq. S4) at the focal plane [1]. Accordingly, the focus pattern should be discussed in the regime of Fraunhofer diffraction. Because the EM field spreads over the square region of the phase-modulating layer and is diffracted out of plane while the shifting of holes induces phase modulation at the same time, it can be ideally considered as the Fraunhofer diffraction pattern of the square aperture at distance $z = f$. Hence, the intensity of the Fraunhofer diffraction pattern of the square aperture is calculated as

$$I(x, y, f) = \frac{A^2}{\lambda^2 f^2} \sin^2 \left(\frac{2w_x x}{\lambda f} \right) \sin^2 \left(\frac{2w_y y}{\lambda f} \right), \quad (\text{S8})$$

where A is the area of the aperture, λ is the wavelength, and w_x and w_y are the respective half-widths of the aperture in the x and y directions [1]. Because the focal spot size is assumed to be the width of the main lobe, which is the distance between the first zero points, it is obtained as

$$\Delta x = \frac{\lambda}{w_x/f}. \quad (\text{S9})$$

Note that this differs from the usual form of the diffraction limit:

$$\Delta x = \frac{\lambda}{\sin(w_x/f)} = \frac{\lambda_0}{n \sin(w_x/f)} = \frac{\lambda_0}{NA}, \quad (\text{S10})$$

where λ_0 is the wavelength in vacuum, n is the refractive index of the propagation medium, and NA is the numerical aperture. This difference is due to the nature of the well-designed imaging lenses used in microscopes. In the case of an imaging lens, the pencils of focusing are assumed to originate from a sphere whose center is at the focus and whose radius is f , as illustrated in Fig. S2(a); this is the so-called sine condition. Meanwhile, in the case of the flat lens in this work, the pencils of focusing are assumed to originate from the plane at the input aperture, as illustrated in Fig. S2(b). Apparently, the sine condition is not satisfied in the latter case. Thus, as mentioned above, the focal spot size should be discussed in terms of Eq. S9. By substituting the parameters $\lambda = 940 \text{ nm}$, $w_x = 100 \mu\text{m}$, and $f = 320 \mu\text{m}$, we obtain the focal spot size for ideal plane-wave incidence as $\Delta x = 3.01 \mu\text{m}$, which is reasonable to consider as a rough estimate of the diffraction-limited spot size.

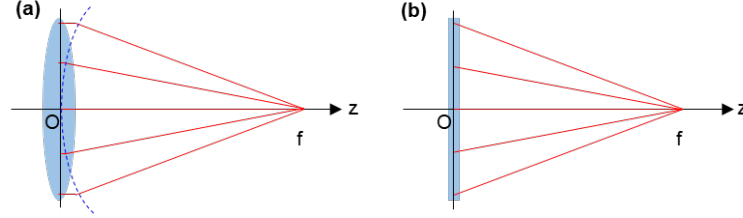


Fig. S2 Schematics of focusing with (a) an imaging lens and (b) a flat lens.

S6 Simple criterion for maximum & minimum focal length

The focal spot size is proportional to the focal length f and inversely proportional to the aperture width w , as described in Eq. S9. Here, the aperture width is relatively small compared to that of an ordinary lens because the iPMSEL was designed to be suitable for integration, so that the range in which focusing occurs by overcoming the spread of diffraction becomes shorter. In fact, the typical width of the emission area in the iPMSEL is on the order of hundreds of micrometers, whereas the width of an ordinary lens is several centimeters. To clarify the focusing property of the iPMSEL, we should discuss the maximum focusing range explicitly. We provide a simple criterion for this purpose as follows. Let us consider the distance at which the focal spot size corresponds to the full width of the input aperture, which is the same as the case of the Fresnel number being 1. The distance is derived from Eq. S9 as

$$f_{\max} = \frac{w^2}{\lambda}, \quad (\text{S11})$$

where w is the half-width of the input aperture. The focal spot size is smaller than the input aperture within this range, so the equation provides a criterion for the maximum focal length. This relationship is visualized at a wavelength of 940 nm in Fig. S2. In this work, the maximum focal length is calculated as 1.06 cm. Note that this only provides a limit on the distance for focusing: the actual focal length should either be set sufficiently shorter than the maximum focal length or determined so as to satisfy the requirement for the focal spot size. If we take the actual focal length to be less than half the maximum focal length, we can roughly estimate that a focal length of several millimeters requires the emission area to have a width of more than 275 μm , as shown in Fig. S3(a). Similarly, Fig. S3(b) shows that a focal length of several centimeters requires the emission area to have a width of more than 870 μm .

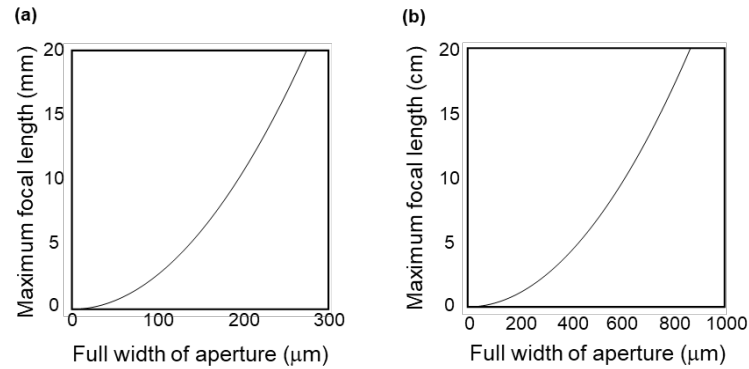


Fig. S3 Dependence of the maximum focal length on the aperture width for (a) a narrow range and (b) a wide range, at a wavelength of 940 nm.

Meanwhile the minimum focal length is considered as following. The smaller the focal length, the higher the phase distribution of each hole, as shown in Eq. (S5). Meanwhile the phase difference between neighboring holes must be below 2π , or it is unable to express the phase

distribution, so that it gives the upper limit of size of the emission area depends on the focal length. According to the Eq. (S5), the phase distribution of the hole at $(x,y)=(w,0)$ is given as

$$\phi_f(w,0) \approx \frac{2\pi}{\lambda} \frac{w^2}{2f}, \quad (\text{S12})$$

while that of the neighboring hole is given as

$$\phi_f(w+a,0) \approx \frac{2\pi}{\lambda} \frac{(w+a)^2}{2f}. \quad (\text{S13})$$

Therefore, the phase difference between neighboring holes is described as

$$\phi_f(w+a,0) - \phi_f(w,0) \approx \frac{2\pi wa}{\lambda f}, \quad (\text{S14})$$

where a is the lattice constant. Because the Eq. S14 must be below 2π , it gives the condition of minimum focal length as

$$\frac{aw}{\lambda} < f. \quad (\text{S15})$$

In the case of the M-point band edge, Eq. S15 can be written as

$$\frac{w}{\sqrt{2}} < f. \quad (\text{S16})$$

References

1. J. Goodman, *Introduction to Fourier Optics*, 3rd ed., Roberts & Co. Publishers (2005).
2. M. Born and E. Wolf, *Principles of Optics*, 7th ed., Cambridge University Press (2011).
3. B. R. Brown and A. W. Lohmann, "Complex spatial filtering with binary masks," *Appl. Optics* **5**(6), 967-969 (1966).
4. Y. Takiguchi, K. Hirose, T. Sugiyama, Y. Nomoto, S. Uenoyama, and Y. Kurosaka, "Principle of beam generation in on-chip 2D beam pattern projecting lasers," *Opt. Express* **26**(8), 10787-10800 (2018).
5. K. Hirose, Y. Takiguchi, T. Sugiyama, Y. Nomoto, S. Uenoyama, and Y. Kurosaka, "Removal of surface-normal spot beam from on-chip 2D beam pattern projecting lasers," *Opt. Express* **26**(23), 29854-29866 (2018).